ELSEVIER

Journal of Alloys and Compounds 320 (2001) 72–79

Journal of ALLOYS AND COMPOUNDS

www.elsevier.com/locate/jallcom

Thermodynamic assessment of the Ru–Si and Os–Si systems

Y.Q. Liu[a,c], G. Shao[a,*], K.P. Homewood[b]

[a]*School of Mechanical and Materials Engineering, University of Surrey, Guildford, Surrey GU2 7XH, UK*
[b]*School of Electronic Engineering, Information Technology and Mathematics, University of Surrey, Guildford, Surrey GU2 7XH, UK*
[c]*Research Center of Physical Chemistry, General Research Institute for Non-ferrous Metals, Beijing, 100088, PR China*

Received 12 October 2000; received in revised form 8 January 2001; accepted 10 January 2001

Abstract

The thermodynamic properties and phase diagrams of the Ru–Si and Os–Si systems are assessed. The calculated enthalpies of fusion and entropies of fusion of ruthenium and osmium silicides are compared with the reported values of different transition metal silicides. Both the thermodynamic properties and the phase diagrams of Ru–Si and Os–Si systems are in good agreement with the available experimental data.

Keywords: Ruthenium–Silicon; Osmium–Silicon; Phase diagrams; Thermodynamic properties; Silicides

1. Introduction

There has been an increasing interest in the transition metal silicides. Their stability and oxidation resistance make these alloys excellent candidates as materials for high temperature applications. Their relatively low electrical resistance has been utilized in microelectronics for the development of integrated circuit technology. Some transition metal silicides exhibit superconducting properties. The ruthenium silicides have been of considerable interest for their possible application as luminescent material in silicon based light emitters (LEDs) and as a promising new material for thermoelectrical applications [1,2]. The osmium silicides are reported to be semiconducting [3]. Despite the great interest in the ruthenium and osmium silicides for electrical and electronic devices, the thermodynamic properties of the Ru–Si and Os–Si systems are still incomplete. Reliable thermodynamic data are essential for assessing and predicting the behavior of these silicides. In this paper, the phase relations and thermodynamic properties of the Ru–Si and Os–Si systems are assessed using the CALPHAD technique.

2. Experimental information

2.1. The Ru–Si system

An early phase diagram of the Ru–Si system was presented by Obrowski [4]. On the basis of metallographic analysis of various alloys, three intermediate phases were observed and were assigned as Ru_2Si_3, RuSi and Ru_2Si. Another phase, Ru_5Si_3, was observed in as-melted samples, but not in annealed ones, by Engström [5]. Weitzer et al. [6] investigated the phase diagram of the Ru–Si system between 1273 and 1603 K using X-ray diffraction and reported five intermetallic compounds: Ru_2Si_3, RuSi, Ru_4Si_3, Ru_5Si_3 and Ru_2Si.

Recently, Perring et al. [7] revised the phase diagram of the Ru–Si system using differential thermal analysis, X-ray diffraction, and electron microprobe investigations. The occurrence of Ru_5Si_3 in Refs. [5,6] was not confirmed. Three eutectic and two peritectic transformations were identified,

E1: liquid=Ru_2Si_3+(Si) at 1573 K, instead of 1643 K in Ref. [6].
E2: liquid=Ru_2Si_3+RuSi at 1953 K, similar to 1963 K in Ref. [6].
E3: liquid=(Ru)+Ru_2Si at 1813 K, instead of 1778 K in Ref. [6].
P1: liquid+Ru_4Si_3=Ru_2Si at 1817 K.

*Corresponding author. Tel.: +44-1483-876-288; fax: +44-1483-876-291.
E-mail address: G.Shao@surrey.ac.uk (G. Shao).

0925-8388/01/$ – see front matter
PII: S0925-8388(01)00931-8

P2: liquid+RuSi=Ru_4Si_3 at 1833 K instead of 1968 K in Ref. [6].

It has been reported that the RuSi exists in two crystal structures: a CsCl-type and a FeSi-type structure. However, the composition range and the relationship between the two forms of RuSi are still in debate. Finnie [8] proposed that the CsCl-type may be stable over only part of the temperature range between 1613 K and room temperature and is slightly more metal-rich than the FeSi-type. Buschinger et al. [9] found a phase transition in stoichiometric RuSi from the high temperature CsCl-structure to the low temperature FeSi-type structure at about 1578 K, with the transition temperature decreasing rapidly with increasing Ru-excess. Perring et al. [10] reported that the stoichiometric RuSi had the CsCl-type instead of the FeSi-type structure at 1515 K. Recently, Perring et al. [7] reported that the two structures coexisted as distinct phases near the equi-atomic composition. The composition ranges of CsCl-type and FeSi-type RuSi measured by electron probe microanalysis are about 47.1–48.2($\pm$0.1) and 49.1($\pm$0.1) at.% Si, respectively. No transformation of the two forms of RuSi was reported at the temperature range 1273 K to 1773 K [7], this is not consistent with the results of [9,10].

In the Ru–Si system, the phase transformation between the two crystal structures of the Ru_2Si_3 (orthorhombic and tetragonal) was reported by Poutcharovsky et al. [11], but the transformation temperature was not well defined. However, the tetragonal Ru_2Si_3 was not detected by [6,7]. In this paper, we only take into account the thermodynamic properties of the FeSi-type RuSi and the orthorhombic Ru_2Si_3.

The thermodynamic properties of the Ru–Si system have been investigated by several researchers. Kuntz et al. [12] determined the molar heat capacity of RuSi and Ru_2Si_3 by differential scanning calorimetry in the temperature range from 310 K to 1080 K. Table 1 summarizes the reported enthalpies of formation of the ruthenium silicides. Meschel and Kleppa [13] measured the enthalpy of formation of RuSi and Ru_2Si_3 using high temperature direct synthesis calorimetry. The enthalpy of formation of RuSi given by Meschel and Kleppa [13] agrees well with the previously determined values by Perring et al. [10] and Topor and Kleppa [14]. The enthalpy of formation of Ru_2Si_3 given by Meschel and Kleppa [13] agrees reasonably with the result of [10]. Perring et al. [10] reported the enthalpy of formation of Ru_4Si_3 at 1505 K using high temperature calorimetry.

Because of the importance of the thermodynamic prop-

Table 1
Comparison of the assessed enthalpies of formation ΔH_f of silicides in the Ru–Si system with some experimental and predicted data reported in the literature

Silicide	ΔH_f, kJ/(mole-atoms)	Method	Ref.
RuSi	−58.3±2.1	High temperature direct synthesis calorimetry	[13]
	−57.7±1.4 (1505 K)	High temperature calorimetry	[10]
	−56.5	–	[12]
	−58.1±3.7	Solute–solvent drop calorimetry	[14]
	−32	Prediction	[15]
	−43.9	Prediction	[16]
	−33.2	Estimation	[17]
	−39.2	Prediction	[18]
	−33.4	–	[19]
	−42	Assessment	[20]
	−33.4	Assessment	[21]
	−56.454	Assessment	This work
Ru_2Si_3	−60.7±1.7	High temperature direct synthesis calorimetry	[13]
	−50.3±1.0 (1704 K)	High temperature calorimetry	[10]
	−49.2	–	[12]
	−26.8	–	[22]
	−26	Prediction	[15]
	−26.8	Estimation	[17]
	−49.060	Assessment	This work
Ru_4Si_3	−45.9±0.6 (1505 K)	High temperature calorimetry	[10]
	−57.561	Assessment	This work
Ru_2Si	−29	Prediction	[15]
	−37.6	Prediction	[16]
	−22.2	Assessment	[21]
	−38.700	Assessment	This work

erties of the transition metal silicides, some models or semi-empirical methods were proposed to predict their enthalpies of formation. Table 1 also shows the enthalpies of formation predicted using the semi-empirical model of Miedema and coworkers [15]. It can be seen that the predicted values are considerably less exothermic than the experimental results of [10,13,14].

Pasturel et al. [16] proposed a model to predict the enthalpies of formation of transition metal silicides and germanides. The authors proposed that the enthalpies of formation of silicides and germanides had two contributions. The first is the energy necessary to convert Si and Ge from the non-metallic into the metallic state and the second is the result of the filling of the d band of the transition metal by the free valence electrons of the metallic Si and Ge. It can be seen that the predicted values of [16] is less exothermic than the experimental results of [10,13,14]. Chart [20] assessed the thermochemical data for transition metal silicides, the results are also shown in Table 1. Until now, no thermodynamic properties of the liquid phase have been reported.

2.2. The Os–Si system

An early phase diagram of the Os–Si system was proposed by Finnie [8]. The eutectic temperature on the silicon-rich side of the Os–Si system was found to be at 1633±15 K [8]. Mason and Muller-Vogt [23] studied the preparation, crystal growth and the physical properties of $OsSi_2$. It was found that the mixture of 15 at.% Os and 85 at.% Si was completely liquid at 1730 K. On slow cooling, $OsSi_2$ crystallized until the eutectic temperature was reached at 1630 K. The eutectic composition was slightly above 90 at.% Si.

The complete phase diagram of the Os–Si system has been investigated by Schellenberg et al. [3] using X-ray powder diffraction, differential thermal analysis, metallography, microprobe analysis and electrical resistivity measurements. Three intermetallic phases existed in this system, OsSi, Os_2Si_3 and $OsSi_2$. Two eutectic and two peritectic transformations were identified:

E1: liquid=(Si)+$OsSi_2$ at 1633 K, consistent with the results of [8,23].
E2: liquid=(Os)+OsSi at 1993 K.
P1: liquid+Os_2Si_3=OsSi at 2003 K.
P2: liquid+Os_2Si_3=$OsSi_2$ at 1913 K.

Table 2 summarizes the reported enthalpies of formation of the osmium silicides. The only experimentally determined thermodynamic data of the Os–Si system is the enthalpies of formation of Os_2Si_3 measured by Meschel and Kleppa [24]. The enthalpy of formation of OsSi given by Topor and Kleppa [14] is estimation only, due to the incomplete dissolution of the compound and components in the solvent used in the solute–solvent drop methods.

Table 2
Comparison of the assessed enthalpies of formation ΔH_f of silicides in the Os–Si system with some experimental and predicted data reported in the literature

Silicide	ΔH_f, kJ/(mole-atoms)	Method	Ref.
Os_2Si_3	−30.5±2.1	High temperature direct synthesis calorimetry	[24]
	−23	Prediction	[15]
	−41.4	Estimation	[17]
	−30.450	Assessment	This work
OsSi	−30~−50	Solute–solvent drop calorimetry	[14]
	−29	Prediction	[15]
	−16.7	Prediction	[16]
	−32.6	–	[19]
	−42	Assessment	[20]
	−32.6	Assessment	[21]
	−25.415	Assessment	This work
$OsSi_2$	−16	Prediction	[15]
	−20.9	Prediction	[16]
	−34.2	Estimation	[17]
	−36.8	Assessment	[21]
	−28.745	Assessment	This work

The predicted values using the semi-empirical model of Miedema and coworkers [15] and the model proposed by Pasturel et al. [16] are also shown in Table 2. No thermodynamic data of the liquid phase has been reported.

3. Thermodynamic model

3.1. Elements

The Gibbs energy of a pure element is taken from Ref. [25], which is referred to as ${}^0H_i^{SER}$, the enthalpy for its stable state at 298.15 K.

3.2. Stoichiometric phases

Since the homogeneity range of the ruthenium silicides and osmium silicides are not well defined, all intermetallic compounds in the Ru–Si and Os–Si systems are treated as stoichiometric phases. The Gibbs energy of a stoichiometric compound ${}^0G_{M_pSi_q}$ is expressed as follows:

$$ {}^0G_{M_pSi_q} = p\,{}^0G_M + q\,{}^0G_{Si} + a + bT + cT\ln T + dT^2 + e/T \quad (1) $$

where, M refers to Ru or Os. ${}^0G_M$ and ${}^0G_{Si}$ are the Gibbs energy of the pure elements M and Si, respectively. *a*, *b*, *c*, *d* and *e* are parameters to be determined.

3.3. Solution phases

For a substitional solution phase ϕ, such as the liquid and hcp–Ru phases, the molar Gibbs energy is equal to

$$G_m^{\phi} = G_m^{ref} + G_m^{id} + {}^{ex}G_m \quad (2)$$

with

$$G_m^{ref} = x_M {}^0G_M + x_{Si} {}^0G_{Si} \quad (3)$$

$$G_m^{id} = RT[x_M \ln x_M + x_{Si} \ln x_{Si}] \quad (4)$$

$${}^{ex}G_m = x_M x_{Si} L \quad (5)$$

where the interaction term L can be composition- and temperature-dependent as follows:

$$L = \sum_{i=0}^{n} (a_i + b_i T)(x_M - x_{Si})^i \quad (6)$$

where, a_i and b_i are parameters to be determined.

4. Evaluation of the thermodynamic parameters

The model parameters are evaluated using the Parrot module in the Thermo-Calc program package [26]. This program is able to take various kinds of experimental data in the operation. It works by minimizing an error sum with each kind of the selected data values, given a certain weight. The weight is chosen and adjusted based on the data uncertainties given in the original publications, until most of the selected experimental information is reproduced within the expected uncertainty limits. All thermodynamic calculations are carried out using the Thermo-Calc program package.

4.1. The Ru–Si system

The enthalpies of formation of different ruthenium silicides are used as a guide for selecting the initial values of interaction parameters. At first, the heat capacity data of Kuntz et al. [12] are used to optimize the parameters of RuSi and Ru_2Si_3 phases. The phase diagram data summarized by [6,7] are used to optimize the parameters of other phases.

4.2. The Os–Si system

The enthalpy of formation of Os_2Si_3 given by Meschel and Kleppa [24] and the predicted enthalpies of formation of OsSi and $OsSi_2$ from the semiempirical model of Miedema and coworkers [15] are used as a guide for selecting the initial values of interaction parameters. The phase diagram data given by Schellenberg et al. [3] are used to optimize the parameters.

5. Results and discussion

By means of the computerized optimization, a complete and self-consistent thermodynamic description for the Ru–Si and Os–Si systems is obtained and listed in Appendix A.

5.1. The Ru–Si system

The calculated molar heat capacity of RuSi and Ru_2Si_3 at different temperatures are shown in Fig. 1(a) and (b), respectively. It can be seen that the calculation results agree well with the experimental values [12].

The calculated enthalpies of formation of ruthenium silicides at 298.15 K are listed in Table 1. All available literature values (experimental, assessed and predicted) are listed in the table. It can be seen that the enthalpy of formation of RuSi calculated in the present work agrees well with the values given by Refs. [10,12–14]. The

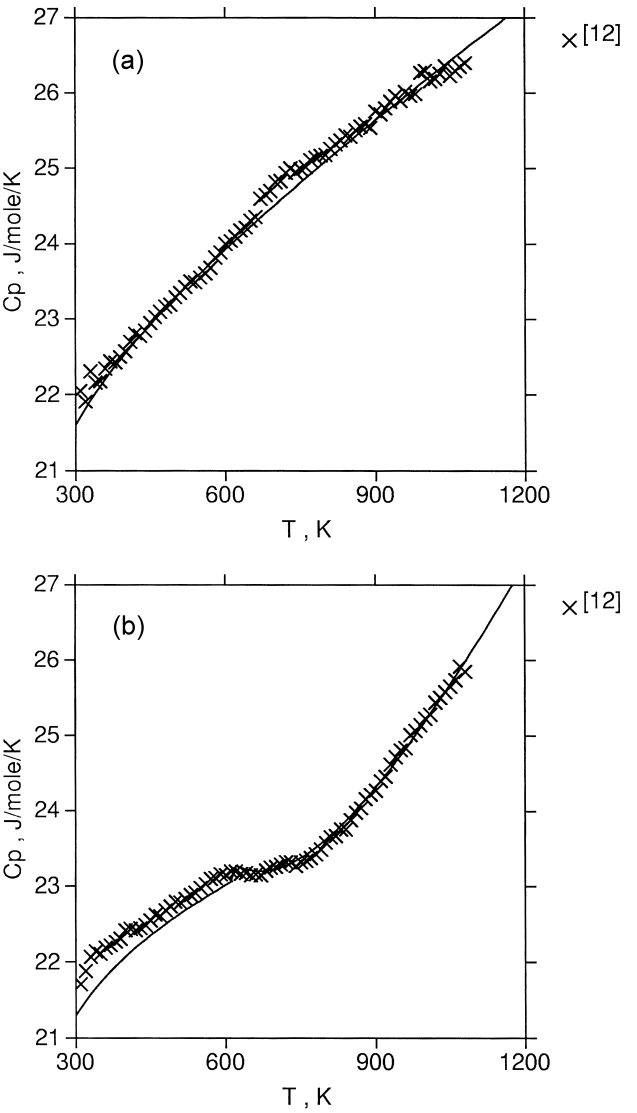

Fig. 1. Calculated heat capacity of RuSi (a) and Ru_2Si_3 (b) at different temperatures, together with experimental data. The heat capacities correspond to one mole of atoms. ×, [12].

calculated enthalpy of formation of Ru_2Si_3 agrees well with the values given by [10,12].

Murarka [27] proposed that the magnitude of the enthalpies of formation of transition metal silicides should increase with increasing silicon content in the alloys, provided that the values are normalized with respect to the number of moles of metal atoms. The calculation results of this work generally agree with this prediction.

Chart [20] pointed out that the entropy of fusion of transition metal silicides versus their melting points obeys the similar trends to those shown by the pure elements [28], that is, there is a correlation between the entropy of fusion and melting point within a group of elements that have a particular crystal structure. The enthalpies of fusion and the melting points reflect the cohesion energy. The relationships between enthalpies of fusion and entropy of fusion of TMSi (TM represents transition metal) vs. melting points are shown in Fig. 2(a) and (b), respectively. The relationships between the enthalpies of fusion and entropy of fusion of TM_2Si vs. melting points are shown in Fig. 3(a) and (b), respectively. The calculated enthalpies of fusion and entropies of fusion of RuSi and Ru_2Si agree reasonably with the general trends.

The calculated phase diagram of the Ru–Si system is compared with various experimental phase boundary data in Fig. 4. Table 3 presents the comparison of the calculated invariant equilibria with the literature values. It can be seen that the calculation agrees well with the experimental data.

It should be pointed out that the reported melting points of RuSi differ greatly, from 2143 K [29], 2023 K [22] to 2003 K [6,30]. Our results show that the values given by [6,22,30] were more reasonable.

5.2. The Os–Si system

The calculated enthalpies of formation of osmium silicides at 298.15 K are listed in Table 2. All available literature values (experimental, assessed and predicted) are listed in the table. It can be seen that the values scatter

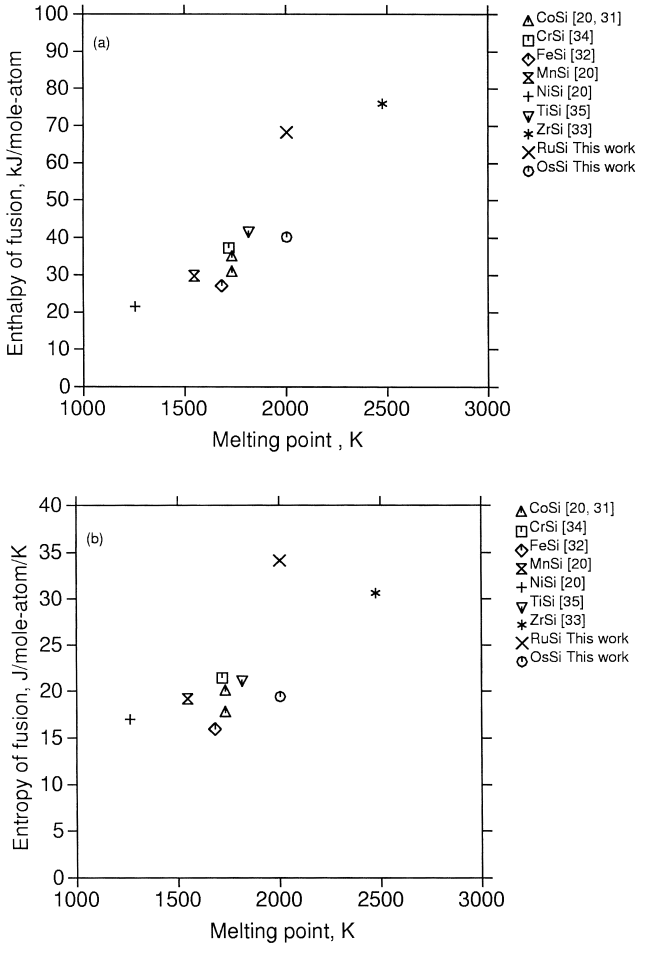

Fig. 2. Correlation of the enthalpy of fusion (a), and the entropy of fusion (b) to the melting point of TMSi, (TM represents transition metal). △ CoSi, [20,31]; ⊡ CrSi, [34], ◇ FeSi, [32]; ⧖ MnSi, [20]; + NiSi, [20]; ▽ TiSi, [35]; ∗ ZrSi, [33]; × RuSi, this work; ⏲ OsSi, this work.

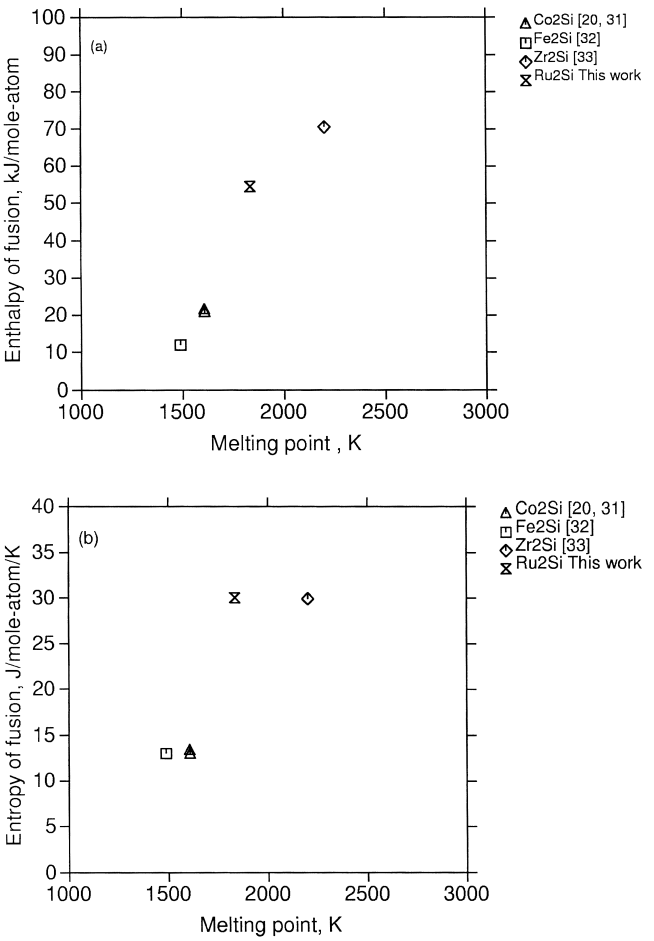

Fig. 3. Correlation of the enthalpy of fusion (a), and the entropy of fusion (b) to the melting point of TM_2Si, (TM represents transition metal). △ Co_2Si, [20,31]; ⊡ Fe_2Si, [32]; ◇ Zr_2Si, [33]; ⧖ Ru_2Si, this work.

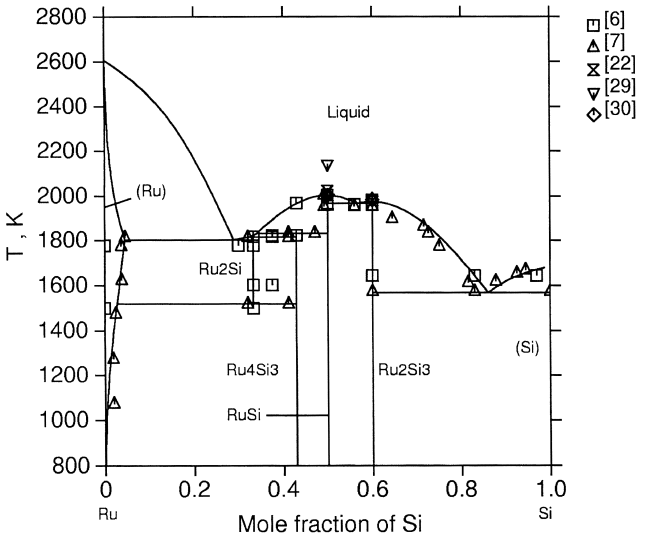

Fig. 4. The calculated phase diagram of the Ru–Si system compared with experimental data. ⊡, [6]; △, [7]; ⧖, [22]; ▽, [29]; ◇, [30].

greatly. The calculated enthalpy of formation of Os_2Si_3 agrees well with the recently determined value of [24].

Similar to the ruthenium silicides, the calculated enthalpies of formation of the osmium silicides increase with increasing silicon content when the data are normalized with respect to the number of moles of osmium atoms. This is consistent with the predictions of Murarka [27].

The calculated enthalpies of fusion and entropy of fusion of OsSi are shown in Fig. 2(a) and (b), respectively. The relationships between enthalpy of fusion and entropy of fusion of $TMSi_2$ vs. melting points are shown in Fig. 5(a) and (b), respectively. The calculated enthalpies of fusion and entropies of fusion of OsSi and $OsSi_2$ are consistent with the general trends.

The calculated phase diagram of the Os–Si system is compared with various experimental phase boundary data in Fig. 6. Table 4 presents the comparison of the calculated invariant equilibria with the literature values. The calculation is in good agreement with the experimental data.

6. Summary

The thermodynamic properties and phase diagrams of the Ru–Si and Os–Si systems are assessed. The calculated enthalpies of fusion and entropies of fusion of ruthenium and osmium silicides are compared with the reported values of different transition metal silicides. Both the

Table 3
Comparison between the calculated invariant equilibria and literature values in the Ru–Si system

Phase reaction	Composition of respective phases, x_{Si}			T (K)	Ref.
liquid = RuSi + Ru_2Si_3	0.55–0.58			1953±10	[7]
	0.56	0.5	0.6	1963	[6,29]
	0.568	0.5	0.6	1968	This work
liquid = Ru_2Si_3 + Diamond	0.83–0.84		1.0	1573±5	[7]
	0.83	0.6	0.97	1643	[6,29]
	0.860	0.6	1.0	1571	This work
liquid + RuSi = Ru_4Si_3				1833±5	[7]
				1968	[6,29]
	0.343	0.5	0.429	1836	This work
liquid + Ru_4Si_3 = Ru_2Si				1817±5	[7]
	0.329	0.429	0.333	1821	This work
liquid = (Ru) + Ru_2Si	0.30–0.31			1813±5	[7]
	0.3			1778	[6]
				1763	[29]
	0.292	0.0452	0.333	1809	This work
Ru_2Si = (Ru) + Ru_4Si_3				1518±5	[7]
				1498	[6]
	0.333	0.0281	0.429	1518	This work
liquid = RuSi				2003	[6]
				2023	[22][a]
				2003	[30]
				2143	[29]
				2004	This work
liquid = Ru_2Si_3				1983	[6,29,30]
				1976	This work

[a] High-temperature phase.

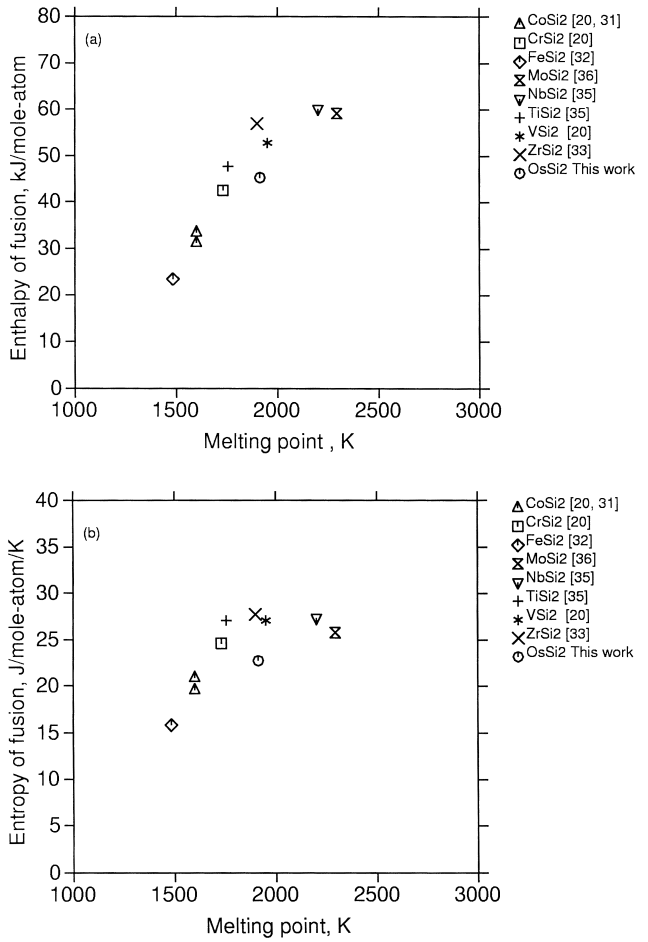

Fig. 5. Correlation of the enthalpy of fusion (a), and the entropy of fusion (b) to the melting point of $TMSi_2$, (TM represents transition metal). △ $CoSi_2$, [20,31]; ⊡$CrSi_2$, [20]; ◇$FeSi_2$, [32]; ⧖$MoSi_2$, [36]; ▽$NbSi_2$, [35]; + $TiSi_2$, [35]; ∗VSi_2, [20]; × ZrSi, [33]; ⏲$OsSi_2$, this work.

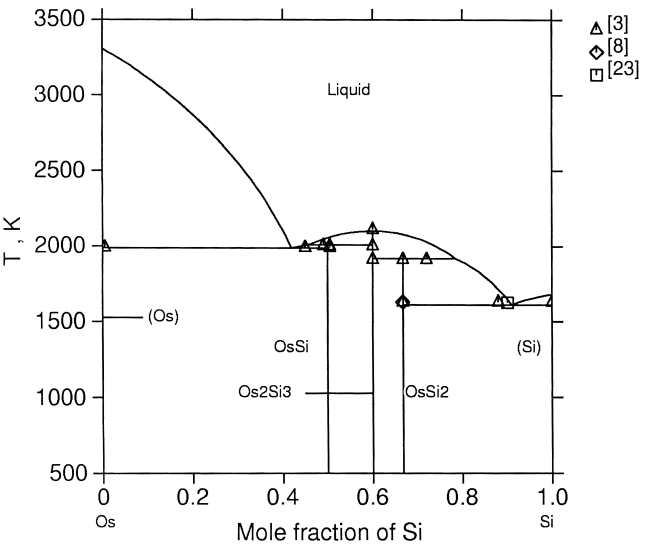

Fig. 6. The calculated phase diagram of the Os–Si system compared with experimental data. △, [3]; ◇, [8]; ⊡, [23].

thermodynamic properties and the phase diagrams of the Ru–Si and Os–Si systems are in good agreement with the available experimental data.

Acknowledgements

Partial financial support of the National Natural Science Foundation of China is acknowledged.

Appendix A

Summary of the optimized thermodynamic parameters for the Ru–Si and Os–Si systems. Values are given in SI units and correspond to one mole of atoms.

The Ru–Si system:

Phase liquid

Description: (Ru, Si)

$$L^{\text{liquid}}_{\text{Ru,Si}} = -127858 - 27.620T + (59628 - 23.850T)(x_{\text{Ru}} - x_{\text{Si}}) + 50985(x_{\text{Ru}} - x_{\text{Si}})^2$$

Phase hcp

Description: (Ru, Si)

$$L^{\text{hcp}}_{\text{Ru,Si}} = -121500 + 15.002T$$

Phase Ru_2Si_3

Description: $(Ru)_{0.4}(Si)_{0.6}$

$$\begin{aligned}{}^0G_{\text{Ru}_2\text{Si}_3} - 0.4\ {}^0G^{\text{hcp}}_{\text{Ru}} - 0.6\ {}^0G^{\text{diamond}}_{\text{Si}} &= -47969 - 24.002T + 1.529T\ \ln T \\ &\quad + 1.026\times10^{-3}T^2 - 81094/T;\ 298.15 < \text{T} \le 620 \\ &\quad - 45010 - 101.091T + 13.745T\ \ln T \\ &\quad - 4.440\times10^{-3}T^2 - 1161172/T;\ 620 < \text{T} < 3000\end{aligned}$$

Phase RuSi

Description: $(Ru)_{0.5}(Si)_{0.5}$

$$\begin{aligned}{}^0G_{\text{RuSi}} - 0.5\ {}^0G^{\text{hcp}}_{\text{Ru}} - 0.5\ {}^0G^{\text{diamond}}_{\text{Si}} &= -55276 - 17.892T + 2.205T\ \ln T \\ &\quad - 6.122\times10^{-5}T^2 - 78350/T\end{aligned}$$

Phase Ru_4Si_3

Description: $(Ru)_{0.572}(Si)_{0.428}$

$${}^0G_{\text{Ru}_4\text{Si}_3} - 0.572\ {}^0G^{\text{hcp}}_{\text{Ru}} - 0.428\ {}^0G^{\text{diamond}}_{\text{Si}} = -57561 + 3.639T$$

Phase Ru_2Si

Description: $(Ru)_{0.667}(Si)_{0.333}$

$${}^0G_{\text{Ru}_2\text{Si}} - 0.667\ {}^0G^{\text{hcp}}_{\text{Ru}} - 0.333\ {}^0G^{\text{diamond}}_{\text{Si}} = -38700 - 1.178T$$

The Os–Si system:

Phase liquid

Description: (Os, Si)

Table 4
Comparison between the calculated invariant equilibria and literature values in the Os–Si system

Phase reaction	Composition of respective phases, x_{Si}			T (K)	Ref.
liquid = Os_2Si_3				2113±20	[3]
				2102	This work
liquid + Os_2Si_3 = $OsSi_2$	0.72±0.02	0.6	0.667	1913±20	[3]
	0.78	0.6	0.667	1921	This work
liquid = $OsSi_2$ + Diamond	0.88±0.01	0.667	1.0	1633±10	[3]
	~0.90			1630	[23]
				1633±15	[8]
	0.90	0.667	1.0	1615	This work
liquid + Os_2Si_3 = OsSi		0.6	0.5	2003±10	[3]
	0.46	0.6	0.5	2011	This work
liquid = OsSi + (Os)	0.45±0.01	0.5	0	1993±10	[3]
	0.42	0.5	0	1988	This work

$$L^{\text{liquid}}_{\text{Os,Si}} = -125865 + 31.560T + (27569 - 11.068T)(x_{\text{Os}} - x_{\text{Si}})$$

Phase hcp

Description: (Os, Si)
$L^{\text{hcp}}_{\text{Os,Si}} = 464047$

Phase OsSi
Description: $(\text{Os})_{0.5}(\text{Si})_{0.5}$
$${}^0G_{\text{OsSi}} - 0.5\ {}^0G^{\text{hcp}}_{\text{Os}} - 0.5\ {}^0G^{\text{diamond}}_{\text{Si}} = -25415 + 1.242T$$

Phase Os_2Si_3
Description: $(\text{Os})_{0.4}(\text{Si})_{0.6}$
$${}^0G_{\text{Os}_2\text{Si}_3} - 0.4\,{}^0G^{\text{hcp}}_{\text{Os}} - 0.6\ {}^0G^{\text{diamond}}_{\text{Si}} = -30450 + 1.805T$$

Phase $OsSi_2$
Description: $(\text{Os})_{0.333}(\text{Si})_{0.667}$
$${}^0G_{\text{OsSi}_2} - 0.333\,{}^0G^{\text{hcp}}_{\text{Os}} - 0.667\ {}^0G^{\text{diamond}}_{\text{Si}} = -28745 + 2.001T$$

References

[1] W. Wolf, G. Bihlmayer, S. Blugel, Phys. Rev. B55 (1997) 6918.
[2] D. Lenssen, D. Guggi, H.L. Bay, S. Mantl, Thin Solid Films 368 (2000) 15.
[3] L. Schellenberg, H.F. Braun, J. Muller, J. Less-Comm. Met. 144 (1988) 341.
[4] W. Obrowski, Metallurgia 19 (1965) 741.
[5] I. Engström, Acta Chem. Scand. 24 (1970) 1466.
[6] F. Weitzer, P. Rogl, J.C. Schuster, Z. Metallk. 79 (1988) 154.
[7] L. Perring, F. Bussy, J.C. Gachon, P. Feschotte, J. Alloys Comp. 284 (1999) 198.
[8] L.N. Finnie, J. Less-Comm. Met. 4 (1962) 24.
[9] B. Buschinger, C. Geibel, J. Diehl, M. Weiden, W. Guth, A. Wildbrett, S. Horn, F. Steglich, J. Alloys Comp. 256 (1997) 57.
[10] L. Perring, P. Feschotte, J.C. Gachon, Thermochim. Acta 293 (1997) 101.
[11] D.J. Poutcharovsky, K. Yvon, E. Parthe, J. Less-Comm. Met. 40 (1975) 139.
[12] J.J. Kuntz, L. Perring, P. Feschotte, J.C. Gachon, J. Solid State Chem. 133 (1997) 439.
[13] S.V. Meschel, O.J. Kleppa, J. Alloys Comp. 274 (1998) 193.
[14] L. Topor, O.J. Kleppa, Z. Metallk. 79 (1988) 623.
[15] F.R. de Boer, R. Boom, W.C.M. Mattens, A.R. Miedema, A.K. Niessen, Cohesion in Metals: Transition Metal Alloys, North-Holland Physics Publishing, 1988, p. 447, p. 595.
[16] A. Pasturel, P. Hicter, F. Cyrot-Lackmann, Physica 124B (1984) 247.
[17] C.S. Petersson, J.E.E. Baglin, J.J. Dempsey, F.M. d'Heurle, S.J. La Placa, J. Appl. Phys. 53 (1982) 4866.
[18] E.S. Machlin, Calphad 5 (1981) 1.
[19] R. Pretorius, J.M. Harris, M.-A. Nicolet, Solid-State Electronics 21 (1978) 667.
[20] T.G. Chart, High Temperatures–High Pressures 5 (1973) 241.
[21] A.W. Searcy, L.N. Finnie, J. Am. Ceram. Soc. 45 (1962) 268.
[22] R.W. Mann, L.A. Clevenger, in: K. Maex, M. van Rossum (Eds.), Properties of Metal Silicides, INSPEC, 1995, p. 56.
[23] K. Mason, G. Muller-Vogt, J. Crystal Growth 63 (1983) 34.
[24] S.V. Meschel, O.J. Kleppa, J. Alloys Comp. 280 (1998) 231.
[25] A.T. Dinsdale, Calphad 15 (1991) 317.
[26] B. Sundman, B. Jansson, J.O. Andersson, Calphad 9 (1985) 153.
[27] S.P. Murarka, Mater. Lett. 1 (1982) 26.
[28] A.P. Miodownik, in: O. Kubaschewski (Ed.), Metallurgical Chemistry, HMSO, London, 1972, p. 233.
[29] E. Savitsky, V. Polyakova, N. Gorina, N. Roshan, in: Physical Metallurgy of Platinum Metals, MIR Publications, Moscow, 1978, p. 161.
[30] T.B. Massalski, in: 2nd Edition, Binary Alloy Phase Diagrams, Vol. 3, ASM, 1990, p. 3253.
[31] S.D. Choi, Calphad 16 (1992) 151.
[32] Z.-K. Liu, Y.A. Chang, Metall. Trans. A 39A (1999) 1081.
[33] C. Gueneau, C. Servant, I. Ansara, N. Dupin, Calphad 18 (1994) 319.
[34] C.A. Coughanowr, I. Ansara, Calphad 18 (1994) 125.
[35] H. Liang, Y.A. Chang, Intermetallics 7 (1999) 561.
[36] Y. Liu, G. Shao, P. Tsakiropoulos, Intermetallics 8 (2000) 953.